ISSN 2347 - 3983
Volume 10. No.1, January 2022
International Journal of Emerging Trends in Engineering Research
Available Online at http://www.warse.org/IJETER/static/pdf/file/ijeter021012022.pdf
https://doi.org/10.30534/ijeter/2022/021012022

Effect of Microstructure Evolution and Corrosion Behavior on Phase Transformation of Nanocrystalline SUS304 Prepared by Dry Ice Shot Peening

Muhammad Rifai[1], Mujamilah[1], Hiroyuki Miyamoto[2]
[1]Center for Research and Technology of Nuclear Advanced Material, National Research and Innovation Agency, Serpong, Tangerang Selatan, Banten, Indonesia
[2]Department of Mechanical Engineering, Doshisha University, 1-3 Tatara Miyakodani, Kyotanabe, Kyoto 610-0394, Japan

Received Date December 04, 2021 Accepted Date : December 29, 2021 Published Date : January 07, 2022

ABSTRACT

Microstructure and corrosion behavior of nanocrystalline SUS304 by dry ice shot peening has been investigated in detail in term of phase transformation. SUS304 as metastable austenitic stainless has excellent corrosion resistance and induced martensite by shot peening process. However, the SUS304 has quite low strength which is difficult to wear as metallic component. The dry ice shot peening process was carried out on SUS304 surface for one and three hours. The microstructure was observed by transmission electron microscope (TEM) and scanning electron microscope (SEM) equipped with electron back-scattered diffraction (EBSD). The phase transformation was analyzed by X-ray diffraction (XRD). The corrosion testing was carried out in 3.5% NaCl solution. The result indicated that the grain size of SUS304 surface was finer by deformation due to dry ice shot peened process. The hardness was improved properly by the increasing the shot peened time, and the corrosion resistance was increased. The XRD results showed that three hours shot peening process induced martensite phase of SUS304 by 15 μm thickness. It can be summarized that the dry ice shot peening can be induced phase transformation due to high deformation on the SUS304 surface.

Key words: Microstructure; corrosion; grain refinement, SUS304

1. INTRODUCTION

SUS 304 stainless steel is well known for the corrosion resistance for industrial and daily life application, but they have weakness at their mechanical properties [1-6]. The high corrosion resistance is occurred due to nickel and chromium contents in the SUS 304 [7-12]. The chromium produces passive layer on the stainless steel to protect from acidic environment. Phase transformation at SUS 304 is induced when the material was treated a deformation, such as a shot peening process [13-16]. The shot peening process improve the mechanical properties on the material surface [17-20]. The deformation which applied on the surface material introduced the phase transformation on SUS 304, its occurred due to the stacking fault energy (SFE) and grain boundary defect [19, 20]. The SUS 304 surface was modified by grain refinement process for around micrometer scale on the surface. The diffusion process is occurred at the grain boundary due to high dislocation density and energy stored inside grain and grain boundaries [21-23]. The phase transformation of martensite is quite easier to occur due to high diffusion process at SUS 304 by shot peening [24-28]. This study purpose is to investigate the phase transformation of SUS 304 due to severe plastic deformation by shot peening in term grain refinement, crystal structure, microstructure evolution and corrosion behavior.

2. EXPERIMENTAL PROCEDURE

Table 1: Chemical composition of SUS304

mass%

	C	Si	Mn	P	S	Ni	Cr	Fe
SUS304	0.08	1.00	2.00	0.045	0.030	8	18	Bal.

SUS304 austenitic stainless-steel sample was use in this investigation, having a chemical composition in table 1. This material was machined with dimensions of 20 × 20 × 2 mm for shot peening. The sample have been exposed to severe plastic deformation via shot peening by dry ice. The mounted specimen was ground with abrasive papers from number 240 until number 2000 and then polished with buff paper with alumina suspension (PRESI) 9, 3 and 1 μm. For the last step of the polishing process, an OP-S suspension (Struers) was used. A scanning electron microscope of field-emission type (FE-SEM, JSM 7001F), equipped with electron back-scattered diffraction (EBSD, Oxford Instrument Co.) image was used to observe orientation map of grains. EBSD orientation maps were processed using INCATM software. A field-emission transmission electron microscope (FE-TEM, JEM 2100F) was used to examine the microstructures. Thin foils for TEM were polished using abrasive papers to about

100 μm thick and then thinned by a twin-jet polishing Tenupol 5 facility (Struers Co., Ltd.) using a solution of 40% acetic acid, 30% phosphoric acid, 20% nitric acid, and 10% distilled water. X-ray diffraction (XRD) on shot peened and post annealed sample was carried out by SmartLab, Rigaku. XRD sample surfaces were buffed by an automatic polisher. The SmartLab X-ray diffractometer used CuKα 40kV, and 0.2A from 40 until 100 deg with continuous scanning type. Full width half maximum (FWHM) was determined after fitting the scattered XRD data. Anodic polarization testing was carried out in neutral solutions containing 1 mol/L NaCl at room temperature, using a potentiostat HZ5000 (Hokuto Denko, Tokyo, Japan) at a scan rate of 20 mV/min, a corrosion current and an Ag/AgCl reference electrode in a 3 mol/L KCl solution (representing a saturated solution). Each sample was immersed in the etchant solution for one hour. Dissolved oxygen was removed from the solution with argon gas before corrosion testing. Mechanical properties of shot peened and post-annealed were investigated by nano indentation experiments using Nano Indenter G200 (Agilent Technologies, USA). The nano indenter applied 100 mN and 50 μN maximum load on cross section of shot peened sample with a Berkovich three-sided diamond pyramid with centerline-to-face angle 65.3 °and a 20 nm radius at the tip of the indenter.

3. RESULT AND DISCUSSION

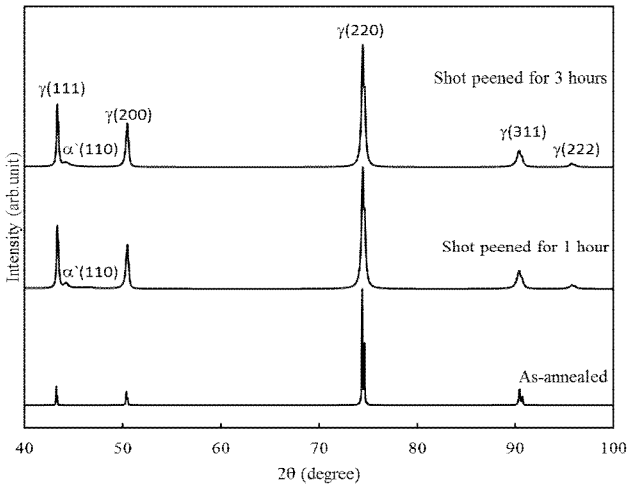

Figure 1: The XRD pattern of as annealed, 1 and 3 hours shot peened sample.

Table 2: XRD line broadening of as-annealed, 1 hour and 3 hours shot peening by dry ice.

Orientation	2θ (degree)	FWHM		
		As annealed	1 hour shot peening	3 hours shot peening
(111)γ	43.660 ± 0.005	0.044 ± 0.001	0.089 ± 0.008	0.122 ± 0.002
(110)α	44.35 ± 0.06	-	0.79 ± 0.08	0.84 ± 0.06
(200)γ	50.817 ± 0.003	0.074 ± 0.005	0.0623 ± 0.0001	0.193 ± 0.002
(220)γ	74.742 ± 0.008	0.091 ± 0.003	0.101 ± 0.001	0.214 ± 0.003
(311)γ	90.703 ± 0.002	0.114 ± 0.007	0.1081 ± 0.0004	0.240 ± 0.004

XRD result shows as-annealed, shot peened for one and three hours, as seen in Figure 1. The phase transformation was occurred in the surface of SUS304L by dry ice shot peening for one and three hours. The transformation from austenite to martensite appears in 110 peaks, and broader after longer time of shot peening process. The broader of 110 peak also indicate the higher defect and lattice distortion occurred in the surface by dry ice shot peening.

Laser microscope observation exhibited roughness of the as-annealed and shot peened surface, as seen in Figure 2. The time of dry ice shot peening process influence to the surface roughness. Figure 2 (c) shows rougher surface for three hours shot peened, it means the dry ice shot peening show similar behavior like common shot peening process. Figure 3 shows orientation, pattern image and phase map for as-annealed and three hours shot peened. The three hours shot peened exhibited higher fraction of martensite. The yellow and pink colors refer to austenite and martensite, respectively. The phase transformation during dry ice shot peening from austenite to martensite is also occurred due to higher diffusion kinetic in martensite.

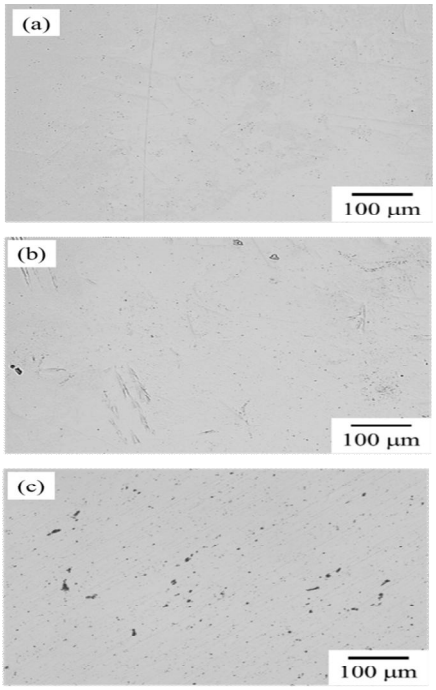

Figure 2: Surface appearance of (a) as annealed, (b) 1, and (c) 3 hours shot peened sample.

Table 3: Surface roughness parameter of as annealed and shot peened sample.

	As annealed	1 hour shot peening	3 hours shot peening
Ra	0.70 ± 0.15	0.50 ± 0.15	3.80 ± 0.23
Rz	3.90 ± 0.66	4.70 ± 1.85	18.70 ± 2.15

Ra: Arithmetic mean height

Rz: Maximum height

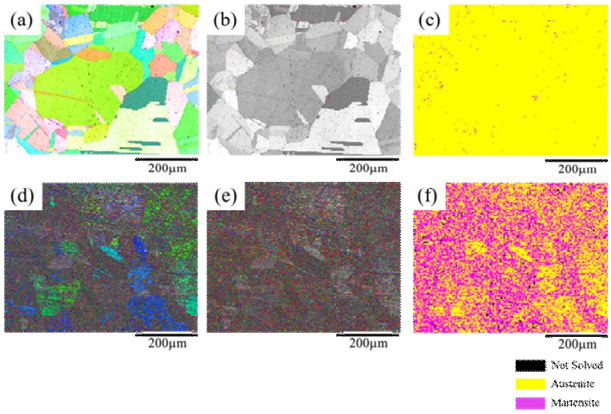

Figure 3: EBSD pattern and phase map of as annealed, and 3 hours shot peened sample.

Texture observation by pole figure was measured by EBSD analysis for one and three hours dry ice shot peened, as seen in Figure 4. The texture shows the {100}, {110} and {111} pole figures for austenite and martensite. The martensite grains show ⟨111⟩ preferred orientation parallel to the peening direction for three hours shot peened sample. The transformation from {110} oriented austenite grains to {111} oriented martensite grains is observed by pole figure obviously, which means the physical parameter could affect to orientation of the material. The deformation by dry ice shot peened influence the texture of the material, especially in the {111}. The higher martensite appearance is occurred due to localized strain by dry ice shot peening process in the SUS304L surface. The texture data by EBSD can complete the XRD data eventually that exhibited phase transformation due to dry ice shot peening on the surface. The higher kinetic energy is promoted by higher deformation level which also induce the phase transformation.

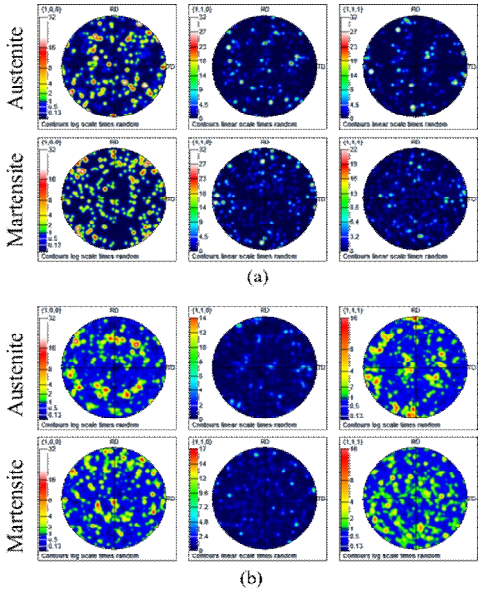

Figure 4: Texture of cross section on 3 hours shot peened and post-annealed sample.

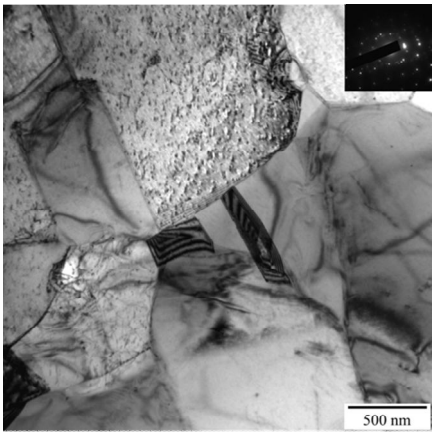

Figure 5: TEM bright field image and SAED pattern of 3 hours shot peened-post annealed sample.

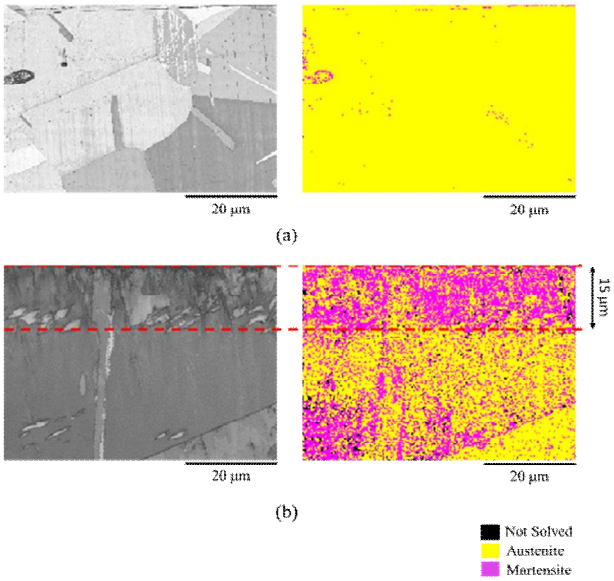

Figure 6: Phase map of cross section on 3 hours shot peened and post-annealed sample.

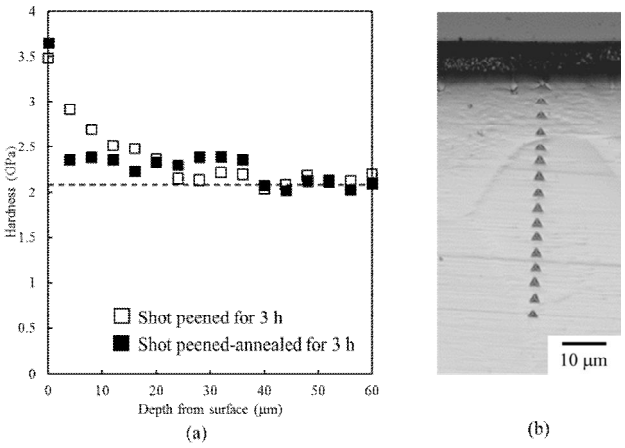

Figure 7: Nano indentation on cross section on 3 hours shot peened and post-annealed sample.

Figure 5 shows the TEM image of three hours shot peened sample. The TEM observation was observed in the normal plane which can observe the mechanical twin, stacking fault and dislocation appearance in the SUS304L during dry ice shot peening process. The selected area electron diffraction shows grain refinement and martensite appearance. The mechanical twin is occurred due higher plastic deformation.
Figure 6 shows cross-section observation of as-annealed and three hours shot peened sample. The yellow and pink color refers to austenite and martensite phase. After three hours shot peening process, the phase map is quite different in surface area, it become martensite with 15 μm thickness. This cross section can be used to identify the strain-induced martensite due to high deformation in the surface and sub-surface.
Figure 7 shows the hardness of the shot peened cross section by nano-indentation. The three hours shot peened exhibited a smooth decrease from 0 to 15 μm in depth, and it is stable to the hardness of the bulk material. It concluded that the martensite is appears until sub-surface due to high deformation until the interior of material. The graph also shows comparation between shot peened for three hours and shot peened-annealed for three hours. It seems the heat treatment process does not change the martensite phase in the surface. The nano-indentation can be used to confirm that plastic deformation influences the microstructure and mechanical properties by dry ice shot peening process.

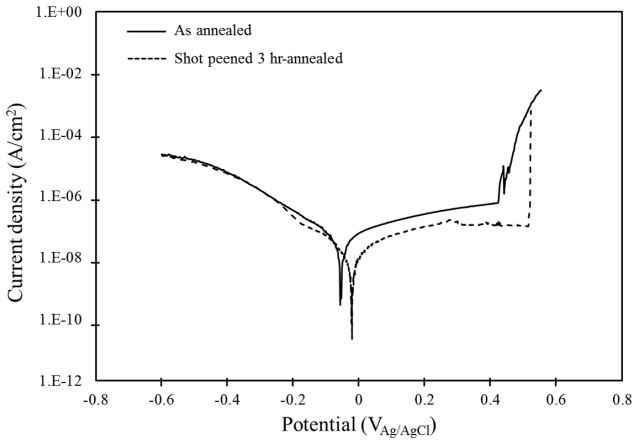

Figure 8: Anodic polarization of the 3 hours shot peened and post-annealed sample.

Figure 8 shows the corrosion behavior of as-annealed and three hours shot peened by potentiodynamic polarization in 3.5% NaCl solution. The shot peened sample exhibited higher corrosion potential than as-annealed sample due to the corrosion kinetics evolution after shot peening process. The result confirmed that the dry ice shot peening improve the corrosion properties.
Dry ice shot peening induced the phase transformation from austenite to martensite by high plastic deformation. SUS304L contain low nickel content which also can induce the phase transformation. Figure 9 showed the result of present research on martensite percentage and strain behavior.

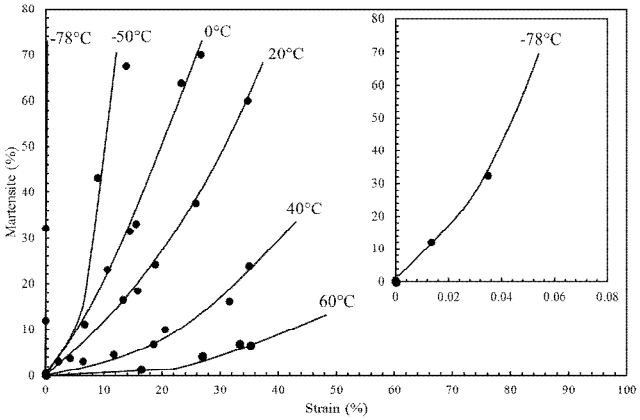

Figure 9: Relationship between martensite and strain with various temperature.

The microstructure is comparable between as-annealed and shot peened material in the sub-surface area, although the high deformation occurred on the surface of shot peened sample. The microstructure of shot peened showed the cell formation and mechanical twin due to high pressure during shot peening process. It can be confirmed by small grain appearance at TEM micrograph. The recrystallization process was partly occurred on the SUS304L`s surface due to accumulation of localized dislocation. The high dislocation density and plastic strain also considered to lead the phase transformation by cyclic hardening at shot peening process. Local cyclic deformation by shot peened process promote the high plastic strain on the surface by dry ice, and it becomes hardened on the surface and sub-surface. The results confirmed that the shot peening process as mechanical surface treatment influenced the microstructure and electrochemistry of the material.

4. CONCLUSION

Effect of strain energy on corrosion behaviour of UFG copper prepared by severe plastic deformation was investigated concerning grain size. SSE processed samples exhibited small grain size with high dislocation density and high grain boundaries fraction due to significant deformation levels. The potentiodynamic polarization curves were used to explain the corrosion behaviour of the UFG copper sample, concluding that corrosion current density showed a high value up to eight passes SSE corresponding to the grain boundaries state. In contrast, the corrosion attack might relate to the homogeneous structure.

REFERENCES

[1] M. Yasuoka, P. Wang, K. Zhang, Z. Qiu, K. Kusaka, Y.S. Pyoun, and R. I. Murakami. **Improvement of the fatigue strength of SUS304 austenite stainless steel using ultrasonic nanocrystal surface modification**, *Surface and Coatings Technology*, vol. 218, pp. 93-98, 2013.

[2] H. Li, Z. Chen, Y. Li, T. Takagi, T. Uchimoto, N. Chigusa, and Y. Yoshida. **Dependence of deformation-induced magnetic field on plastic deformation for SUS304 stainless steel,** *International Journal of Applied Electromagnetics and Mechanics*, vol 38, no. 1, pp. 17-26, 2012.

[3] M. Hatano, H. Tsukasaki, A. Kawaguchi, S. Kawaguchi, Y. Kubota, Y. Ishii, and S. Mori. **Strain-induced ε-martensitic transformation and hydrogen embrittlement of SUS304 stainless steel**, *Philosophical Magazine Letters*, vol. 99, no.11, pp. 404-413, 2019.

[4] X. Li, J. Chen, L. Ye, W. Ding, and P. Song. **Influence of strain rate on tensile characteristics of SUS304 metastable austenitic stainless steel**, *Acta Metallurgica Sinica (English Letters)*, vol. 26, no. 6, pp. 657-662, 2013.

[5] M. Hatano, Y. Kubota, T. Shobu, and S. Mori. **Presence of ε-martensite as an intermediate phase during the strain-induced transformation of SUS304 stainless steel**, *Philosophical Magazine Letters*, vol. 96, no.6, pp. 220-227, 2016.

[6] B. Cao, T. Iwamoto, and P. P. Bhattacharjee. **An experimental study on strain-induced martensitic transformation behavior in SUS304 austenitic stainless steel during higher strain rate deformation by continuous evaluation of relative magnetic permeability**, *Materials Science and Engineering: A*, vol. 774, pp. 138927, 2020.

[7] M. Oyaidzu, K. Isobe, and T. Yamanishi. **Effects of tritiated water on passivation behavior of SUS304 stainless steel**, *ECS Transactions*, vol. 50, no. 50, pp. 63, 2013.

[8] S. Rashid, N. Islami, A. K. Ariffin, M. Ridha, and S. Fonna. **The effect of immersion time on the corrosion behavior of SUS304 in brine using half-cell potential measurement**, *Jurnal Teknologi*, vol. *78*, pp. 6-9, 2016.

[9] M. S. Islam, K. Otani, and M. Sakairi, **Corrosion inhibition effects of metal cations on SUS304 in 0.5 M Cl− aqueous solution**, *Corrosion Science*, vol. 140, pp. 8-17, 2018.

[10] R. Wang, Y. Li, T. Xiao, L. Cong, Y. Ling, Z. Lu, C. Fukushima, I. Tsuchitori, and M. Bazzaoui. **Using atomic force microscopy to measure thickness of passive film on stainless steel immersed in aqueous solution**, *Scientific reports*, vol. 9, no. 1, pp. 1-11, 2019.

[11] D. Morrall, H. Yen-Jui, K. Yabuuchi, A. Kimura, and T. Ishizaki. **Corrosion Behavior of Mechanically Alloyed SUS304L with Zirconium Addition in High-Temperature Water**, *Int J Metall Met Phys*, 3, p.026. 2018

[12] B. Zhang, S. Hao, J. Wu, X. Li, C. Li, X. Di, and Y. Huang. **Direct evidence of passive film growth on 316 stainless steel in alkaline solution**, *Materials Characterization*, vol. 131, pp. 168-174, 2017.

[13] M. Okayasu, and S. Tomida. **Phase transformation system of austenitic stainless steels obtained by permanent compressive strain**, *Materials Science and Engineering: A*, 684, pp.712-725. 2017

[14] H. Tsuruta, K. Shimizu, T. Murakami, Y. Kamada, and H Watanabe. **Structural phase transformations of gallium ion irradiated sus304 steel**, *Nippon Kinzoku Gakkaishi/Journal of the Japan Institute of Metals*, vol. 85, no. 6, pp. 239-246, 2021.

[15] T. Shiratori, T. Yoshino, Y. Suzuki, M. Katoh, S. Nakano, and M. Yang. **Deformation and transformation behavior in micropiercing of SUS304**, *Procedia Manufacturing*, vol. 15, pp. 1452-1458, 2018.

[16] Y. B. Das, A. N. Forsey, T. H. Simm, K. M. Perkins, M. E. Fitzpatrick, S. Gungor, and R. J. Moat. **In situ observation of strain and phase transformation in plastically deformed 301 austenitic stainless steel**, *Materials & Design*, vol. 112, pp. 107-116. 2016

[17] H. Soyama. **Comparison between shot peening, cavitation peening, and laser peening by observation of crack initiation and crack growth in stainless steel**, *Metals*, *10*(1), p.63. 2020

[18] Y. H. Chung, T. C. Chen, H. B. Lee, and L. W. Tsay. **Effect of Micro-Shot Peening on the Fatigue Performance of AISI 304 Stainless Steel**, *Metals*, vol. 11, no. 9, pp. 1408, 2021.

[19] Y. F. Wei, J. J. Lee, H. F. Liu, C. C. Tan, and D. T. Ardi, **Surface Integrity Variations of Stainless Steel 304 upon Severe Shot Peening**, *Materials Science Forum*, vol. 1015, pp. 30-35, 2020.

[20] M. Novelli, J. J. Fundenberger, P. Bocher, and T, Grosdidier, **On the effectiveness of surface severe plastic deformation by shot peening at cryogenic temperature**, *Applied Surface Science*, vol. 389, pp. 1169-1174, 2016.

[21] B. Y. Zhang, B. X. Liu, J. N. He, W. Fang, F. Y. Zhang, X. Zhang, C. X. Chen, and F. X. Yin. **Microstructure and mechanical properties of SUS304/Q235 multilayer steels fabricated by roll bonding and annealing**, *Materials Science and Engineering: A*, vol. 740, pp. 92-107, 2019.

[22] N. Sato, T. Yoshino, T. Shiratori, S. Nakano, and M. Katoh. **Accelerative Effects of Diffusion Bonding of Recrystallization with Reversion of Deformation-induced Martensite in SUS304**, *Isij International*, vol. 56, no. 10, pp. 1825-1830, 2016.

[23] M. Katoh, N. Sato, T. Shiratori, and Y. Suzuki. **Reduction of diffusion bonding temperature with**

recrystallization at austenitic stainless steel, *Isij International*, vol. 57, no. 5, pp. 883-887, 2017.

[24] M. Rifai, H. Miyamoto, and H. Fujiwara. **Effects of strain energy and grain size on corrosion resistance of ultrafine grained Fe-20% Cr steels with extremely low C and N fabricated by ECAP**, *International Journal of Corrosion*, 2015.

[25] M. Rifai, H. Miyamoto, and H. Fujiwara. **Effect of ECAP deformation route on the degree of anisotropy of microstructure of extremely low CN Fe-20mass% Cr alloy**, *Metals*, vol. 4, No. 1, pp. 55-63, 2014.

[26] M. Rifai, M. Yuasa, and H. Miyamoto. **Enhanced corrosion resistance of ultrafine-grained Fe-Cr alloys with subcritical Cr contents for passivity**, *Metals*, vol. 8, no. 3, p.149, 2018.

[27] M. Rifai, H. Miyamoto. **Effect of strain energy on the grain growth behaviour of ultrafine-grained iron-chromium alloy by equal channel angular pressing**, *Journal of Mechanical Engineering and Sciences*, vol. 14, no. 3, pp.7049-7057, 2020.

[28] M. Dani, S. Mustofa, S. Parikin, T. Sudiro, B. Hermanto, D. R. Adhika, A. Insani, A. Dimyati, S. H. Syahbuddin, E. A. Basuki, and C. A. Huang. **Effect of Spark Plasma Sintering (SPS) at Temperatures of 900and 950 o c for 5 Minutes on Microstructural Formation of Fe-25Ni-17Cr Austenitic Stainless Steel**, *International Journal of Emerging Trends in Engineering Research*, vol. 8, no. 8, 2020.